PHYSICAL REVIEW A VOLUME 16, NUMBER 5 NOVEMBER 1977

# Study of self-diffusion in dense hydrogen gas by quasielastic incoherent neutron scattering*

S. H. Chen
*Massachusetts Institute of Technology, Cambridge, Massachusetts 02139*

T. A. Postol and K. Sköld†
*Solid State Science Division, Argonne National Laboratory, Argonne, Illinois 60439*

(Received 28 June 1977)

Incoherent quasielastic scattering of neutrons from hydrogen gas has been measured at room temperature and 78°K in a range of pressures from 100 to 2000 atm. We present in some detail the data-reduction procedure which allows us to extract the van Hove self-correction function $S_s(Q,\omega)$. We then extract the linewidth of the self-correlation function by assuming a Lorentzian line shape. By extrapolating to the small-$Q$ limit, we obtain the macroscopic self-diffusion coefficient as a function of density and temperature. We compare the results with the hard-sphere Enskog theory and conclude that there is considerable enhancement over the Enskog values at higher densities.

## I. INTRODUCTION

With the advent of the technique of computer molecular dynamics[1] (CMD) and recent development of the renormalized kinetic theory of dense gases,[2] the problem of self-diffusion in simple dense fluids has seen a renewed interest.[3] Alder, Gass, and Wainwright[4] carried out an extensive CMD study of the velocity-autocorrelation function (VAF) and the self-diffusion coefficient, which is the area of VAF for a system of hard spheres, at a variety of packing fractions. Their results show that at very low densities, the VAF decay exponentially according to the Enskog expression $\exp(-2t/3t_E)$; $t_E$ is the Enskog collision time which is related to the Enskog self-diffusion coefficient $D_E$ by $t_E = 2D_E/3V_0^2$, where $V_0 = (k_B T/M)^{1/2}$ is the thermal speed of the particle.

As the density increases, however, deviation from the Enskog expression becomes apparent in two ways. (We shall henceforth measure the gas density by a dimensionless quantity $\rho^* = n\sigma^3$ where $n$ is the number density and $\sigma$ is the hard-sphere diameter.) For $\rho^* \lesssim 0.7$ the VAF still decays monotonically from unity at $t = 0$ to less than 0.01 in about 20 collision times. However, the decay is exponential only for times less than one collision time. In the intermediate time regime, corresponding to 3–10 collision times, the hard-sphere VAF shows enhancement over the Enskog VAF by as much as 0.02. At long times corresponding to 20 or more collision times the hydrodynamic effects dominate[5] and the test-particle VAF decays asymptotically as $t^{-3/2}$.

Dorfman and Cohen[6] showed that the $t^{-3/2}$ decay at long time comes from the effects of "ring-collision terms" which are not included in the memory function of the hard-sphere Enskog kinetic equation. Physically the ring terms describe processes of repeated collisions of the test particle with a given particle of the surrounding bath particles. These processes have the effect of enhancing the correlation of the velocity of the test particle at one time and the velocities at later times. Mazenko[2] has shown that part of the enhancement of the hard-sphere VAF over the Enskog VAF in the intermediate time regime comes from the same ring-collision terms.

For $\rho^* \gtrsim 0.8$, which approximately corresponds to the triple-point density in argon, CMD studies of both the hard-sphere system[4] and the Lennard-Jones system by Rahman[7] show a negative excursion of the VAF around three collision times. Physically this corresponds to backscattering of the test particle due to interactions with the surrounding particles. Recently, there have been attempts[8] to explain this negative excursion as well in terms of ring collisions. Although the results are encouraging, the quantitative results are inaccurate because of uncontrolled approximations introduced in the calculations.

An instructive picture,[4] which summarizes the discussion above, is obtained if one plots $D/D_E$, where $D$ is the measured self-diffusion coefficient of the hard-sphere system, as a function of $\rho^*$. The curve starts from unity at $\rho^* = 0$ and gradually increases as the density increases up to a certain value ($\rho^* \approx 0.6$). Above this density it decreases again due to the negative excursion of the VAF. In a real system this kind of plot is meaningful only if one can specify an equivalent hard-sphere diameter. Whether this is possible for systems with an attractive part in the intermolecular potential function is still an open question. One might conjecture that at sufficiently high temperature, where the collisions are hard, an equivalent hard-sphere diameter

should be a useful concept.

In this paper we report neutron-incoherent-scattering measurements on gaseous hydrogen at 293 °K and 500, 1000, 1504, and 1946 atm; and at 77.8 °K and 130, 279, 500 and 800 atm. Incoherent neutron scattering is a dynamic probe which couples to the tagged-particle number and current densities at finite wave vectors. One can show[9] that the self-part of the dynamic structure factor $[S_s(Q,\omega)]$ as measured in the incoherent-neutron-scattering experiment is related to a generalized $Q$- and $\omega$-dependent diffusion coefficient by

$$S_s(Q,\omega)=\left(\frac{\beta\hbar\omega}{1-e^{-\beta\hbar\omega}}\right)\frac{1}{\pi}\,\frac{Q^2}{\omega^2}\,\mathrm{Re}[D(Q,\omega)]\,, \tag{1}$$

where

$$D(Q,\omega)=\frac{1}{\beta}\int_0^\infty dt\, e^{-i\omega t} \times\int_0^\beta d\lambda\, j_x(-Q,-i\hbar\lambda)\,j_x(Q,t)\,. \tag{2}$$

$j_x(Q,t)$ is the $Q$th Fourier component of the test-particle current in the $x$ direction and $\beta=1/k_BT$. Our experimental conditions are such that $\beta\hbar\omega \ll 1$, and Eq. (1) can be simplified to

$$S_s(Q,\omega)=(1/\pi)(Q^2/\omega^2)\,\mathrm{Re}[D(Q,\omega)]\,. \tag{3}$$

It is clear from Eq. (2) that the macroscopic self-diffusion coefficient is the $Q\to 0$ and $\omega\to 0$ limit of $D(Q,\omega)$ and that the incoherent neutron scattering therefore measures the nonlocal self-diffusion coefficient.

In a dilute gas, the motion of a test particle can be characterized by a mean free path between collisions $l\simeq(\pi r_0^2 n)^{-1}$, where $r_0$ is the equivalent hard-sphere diameter and $n$ is the number density. A useful way to estimate whether one is in the collision dominated regime is to consider the dimensionless parameter $y$,

$$y^{-1}\sim Ql\sim Q/\pi r_0^2 n\,, \tag{4}$$

which measures the ratio of the mean free path to the "scale of observation" $1/Q$. For a moderately dense system of hard spheres which is describable by the Enskog theory this parameter can be conveniently defined as

$$y^{-1}=Qr_0/3.342\,nr_0^3 g(r_0)\,, \tag{5}$$

where $g(r_0)$ is the pair-correlation function at contact. The definition of parameter $y$ is in the spirit of the Enskog picture in which the effective collision rate of the test particle is given as $nr_0^2 g(r_0)\times(k_BT/m)^{1/2}$ to account for the nonlocal nature of the hard sphere collision and the local packing of nearest neighbors. Using the Enskog expression for the self-diffusion coefficient[10]

$$D_e=(3/8\sqrt{\pi})(V_0/nr_0^2)[1/g(r_0)]\,, \tag{6}$$

we may also write

$$y^{-1}=\sqrt{2}\,QD_E/V_0\,. \tag{7}$$

From this definition it can be shown[11,12] that $y\geq 2$ corresponds to the collision-dominated (hydrodynamic) regime where the scattering function has a Lorentzian shape

$$S_s(Q,\omega)=(1/\pi)DQ^2/[(DQ^2)^2+\omega^2]\,. \tag{8}$$

$y\ll 1$ corresponds to the free-streaming regime where the scattering function is a Doppler-broadened Gaussian:

$$S_s(Q,\omega)=(\sqrt{2}\,QV_0)^{-1}\exp(-\omega^2/2Q^2V_0^2)\,. \tag{9}$$

It is interesting to note that the limiting behavior described by Eq. (9) is reached for a value of $y$ which is density and temperature dependent.[12] For example, for $\rho^*=0.3$, $T^*=2.15$, free streaming is observed when $y\leq 0.1$, while for $\rho^*=0.84$, $T^*=0.68$, free streaming is observed for $y\leq 0.5$.

Our experimental data cover $y$ values which are both larger and smaller than unity. However, we deduce the diffusion coefficient only from data which correspond to $y\geq 2$.

In Sec. II we discuss the incoherent scattering of neutrons from hydrogen molecules. In Sec. III A we describe experimental details and in Secs. III B and III C we describe the data reduction and multiple-scattering corrections. In Sec. IV we discuss the results of the data analysis and in Sec. V we present our conclusions.

## II. NEUTRON SCATTERING FROM HYDROGEN MOLECULES

Since hydrogen is a diatomic molecule, the double-differential incoherent-neutron-scattering cross section contains contributions from translational, rotational, and vibrational motions of the molecule. Since the first vibrational state of hydrogen is at 540 meV, essentially all molecules will be in their ground-vibrational state at room temperature. Hence the incident 5.2-meV neutrons can neither deexcite nor excite the level. However, at room temperature, the $J=1$ and the $J=2$ rotational states (14.7 and 44.1 meV, respectively) are populated, and the $J=2$ state has about 11% of the total population. It scatters coherently, however, and has a cross section 30 times smaller than the scattering from molecules in the $J=1$ state. Therefore, the conditions for the present experiment are such that we need consider only scattering from molecules in the $J=0$ and $J=1$ states; the cross section can then be written[13]

$$\frac{d^2\sigma}{d\Omega d\omega} = \left(\frac{d^2\sigma}{d\Omega d\omega}\right)_{1\to 1} + \left(\frac{d^2\sigma}{d\Omega d\omega}\right)_{0\to 0} + \left(\frac{d^2\sigma}{d\Omega d\omega}\right)_{1\to 0} . \quad (10)$$

The first two terms in Eq. (10) correspond to scattering which is elastic with regard to internal molecular modes and the line shape is determined by the translational motion of the molecules. The third term is the "inelastic"-scattering component and involves the rotational ortho → para de-excitation. Aside from its small magnitude, this component is well separated ($\Delta E = 14.7$ meV) from the quasielastic peak. Therefore, as far as the quasielastic scattering is concerned, we need consider only the first two terms in Eq. (10) and the cross section can be written

$$\frac{d^2\sigma}{d\Omega d\omega} = a_{\text{inc}}^2 \frac{k_f}{k_i} [j_0^2(Qb) + 2j_2^2(Qb)] S_s(Q,\omega) , \quad (11)$$

where $2b = 0.75$ Å is the internuclear distance of the hydrogen molecule, $k_f$ and $k_i$ are the final and initial wave vectors, respectively, and $a_{\text{inc}}$ is the incoherent-neutron-scattering length. For $Q \leq 1$ Å$^{-1}$ the $j_0$ and $j_2$ spherical Bessel functions have small enough argument that they can, to a good approximation, be replaced by unity and zero respectively. We thus see that the hydrogen molecule offers a convenient possibility to study translational motion without the additional complications due to the rotational degrees of freedom.

## III. THE STUDY

### A. The experiment

The experiment was performed at the Argonne hybrid time-of-flight spectrometer.[14] A pair of graphite monochromator crystals were used to select the energy of the incident neutrons and the beam was modulated by either a Fermi chopper or by a statistical chopper. The detectors were arranged on an arc at scattering angles from $-9.0°$ to $-2.4°$ and $2.4°$ to $9.0°$ at intervals of $0.6°$ giving a $Q$ resolution of about 0.01 to 0.02 Å$^{-1}$ for 4-Å neutrons. Additional detectors at angles higher than $9.0°$ were arranged at intervals of $1.2°$.

Two series of measurements were made. The first series was on hydrogen at room temperature and at $p = 500$, 1000, 1504, and 1946 atm. The incident energy was 5.181 meV and a Fermi chopper was used. Scattered neutrons were detected at 31 angles in the range $-9°$ to $+20.4°$ spaced as described above and "covering" a range of momentum transfers from 0.0662 to 0.560 Å$^{-1}$ for elastically scattered neutrons.

The sample container is illustrated in Fig. 1. The flange on the bomb was machined from 304 stainless steel. It was bolted to the 7075-T651 aluminum pressure jacket with 6 $\frac{1}{4}$–20 Alloy steel screws. A Teflon O-ring was used to seal the gap between the steel flange and the aluminum jacket. The sample was loaded into the container

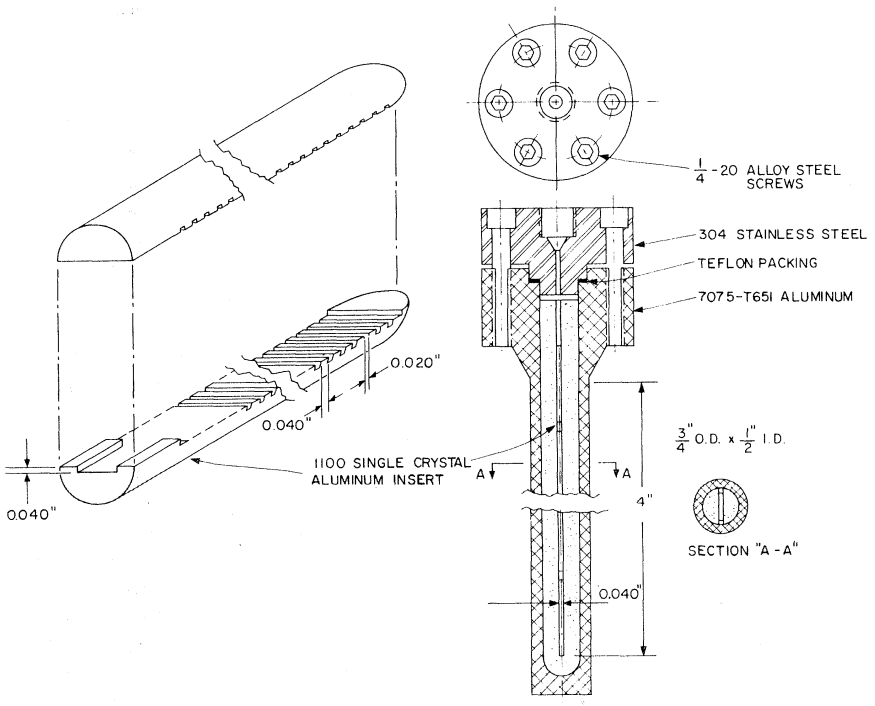


FIG. 1. Sketch of the sample container and the single-crystal aluminum insert.

through 10-mil-o.d. and 8-mil-i.d. stainless-steel tubes of the type used in the manufacturing of hypodermic needles. The tubes were inserted into $\frac{1}{8}$-in.-coned high-pressure fittings and were hard soldered to make a seal.

A single-crystal aluminum spacer was constructed in order to subdivide the gas sample into horizontal square prisms; a diagram of the aluminum spacer is shown in Fig. 1. The aluminum spacer was machined from a single crystal of aluminum into two incomplete half-cylinders which when rejoined resulted in a 40-mil gap parallel to the cylinder length. The gap was further subdivided into horizontal parallel pipeds 40 mil on a side by appropriately spaced 20-mil ribbons of cadmium which were inserted into the flat faces of each half-cylinder. The half-cylinders were cut at a rate of no greater than 10 mil at a time. The crystal was then etched to remove 15 mil of polycrystalline surface. As we will discuss in Sec. III B the insert proved to be an effective method

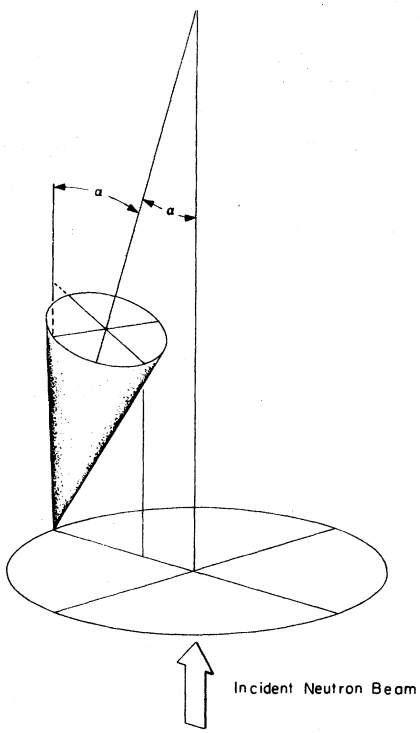


FIG. 2. Geometry of double-Bragg scattering is shown above; neutrons first backscatter into a cone of angle $\alpha = 21°$ and then forward scatter into a second cone of the same angle. All the cones which result from second scattering have a section which contributes some neutrons into the forward direction no matter where they lie on the first cone. As one goes to higher angles, fewer cones contribute neutrons from the double scattering and one sees a sharp decrease in container scattering.

of limiting the gas dimensions to a geometry such that the multiple scattering was reduced to an insignificant level.

The gas-handling system was constructed from standard components from High Pressure Co., 1222 Linden Ave., Erie, Pa. 16505 and the pressure was monitored with a BLH Electronics (Waltham, Mass.) 0–30 000-psi strain-gauge pressure transducer. A 10-V constant-voltage source was used as the strain-gauge reference voltage and the signal was monitored with a Keithley digital voltmeter; the pressure was measured with an accuracy of 0.1%.

Since 5.181-meV neutrons have a wavelength of 3.973 Å it is possible to satisfy the conditions for the (200) and the (111) Bragg reflections in the aluminum container. For the (111) reflection 3.973-Å neutrons will be Bragg scattered at 159°. These neutrons will in turn be Bragg scattered into the forward direction. The angular distribution of these elastically scattered neutrons is shown in Fig. 2. At small angles, intense forward scattering was observed which was strongly dependent on the scattering angle and which we believe was due to multiple Bragg reflection of this kind.

The container scattering proved so severe that it could not be reliably subtracted from the low-angle data. In addition, for the lower densities the ratio of container scattering to sample scattering was so large that the 500-atm data were rendered useless at all angles.

The lower-temperature data were obtained using a statistical chopper in order to increase the signal-to-noise ratio. The statistical chopper substantially improved the accuracy of the measurements and data like those shown in Fig. 7 are typical. The measurements with the statistical chopper used 4.534-meV incident neutrons which have a wavelength of 4.248 Å. Data were accumulated at 15 angles in the range $-8.7°$–$30.6°$ covering a range of momentum transfers from 0.07 to 0.781 $Å^{-1}$ for elastically scattered neutrons. For these measurements the container walls were machined down from $\frac{3}{16}$ to $\frac{1}{8}$ in. in order to take advantage of the greater strength of aluminum at liquid-nitrogen temperature. In addition, longer-wavelength neutrons were used in the hope of avoiding the (200) aluminum-container scattering. Intense forward scattering was still encountered and seemed to be reduced only by the ratio of the wall thicknesses. Because of the difficulty of properly subtracting the container scattering at small angles and the narrower linewidths expected at lower temperatures and higher densities, we chose larger scattering angles in order to minimize the effects of container scattering and instrumental

resolution on the measurement. This choice was possible because the hydrodynamic regime extends to larger values of $Q$ at the lower temperatures.

### B. Data reduction

The information that is obtained from a neutron-scattering experiment is the scattering function $S_s(Q,\omega)$ which is related to the double-differential scattering cross section by

$$\frac{d^2\sigma}{d\Omega d\omega} = a_{\text{inc}}^2 \left(\frac{k_f}{k_i}\right)^{1/2} S_s(Q,\omega). \tag{12}$$

Standard data-reduction procedures[15] were used to derive the scattering function from observed time-of-flight spectras.

The diffusion constant was obtained by fitting a Lorentzian [see Eq. (8)] to the experimental scattering function. We found that the fitted value of the diffusion constant was extremely sensitive to the container subtraction procedure and we were not able to establish any consistent method for fitting the data at small angles reliably; these data were therefore rejected (see also discussion above).

In order to calculate the energy-dependent self-shielding of the sample the removal cross section as a function of energy is needed. The removal cross section was obtained in the course of calculations of the multiple-scattering contribution. These calculations are discussed below and the removal cross section is shown in Fig. 5. As we did not know the exact ortho-para ratio of the sample we were unable to calculate this correction precisely. In order to evaluate the importance of this source of error we calculated the self-shielding correction for various assumed ortho-para ratios and derived the diffusion constant from the resulting scattering function. For example, for the data at 1000 atm we fit the diffusion coefficient using 0.75 and 1.50 times the nominal value of the removal cross section. This increased the skewing of the curve from 2.5% to 5.0% but changed the fitted value of the diffusion coefficient by no more than 2%. Thus, even if the calculated removal cross section were off by as much as a factor of 2, the resulting self-shielding correction would affect the value obtained for the diffusion coefficient by no more than 2%.

We therefore came to the following conclusions in our data analysis: (i) that we could not reliably subtract the container scattering; (ii) that sample self-shielding effects were not significant in introducing errors in the measured diffusion coefficient.

We therefore fit the data by suppressing all points where significant elastic container scatter-

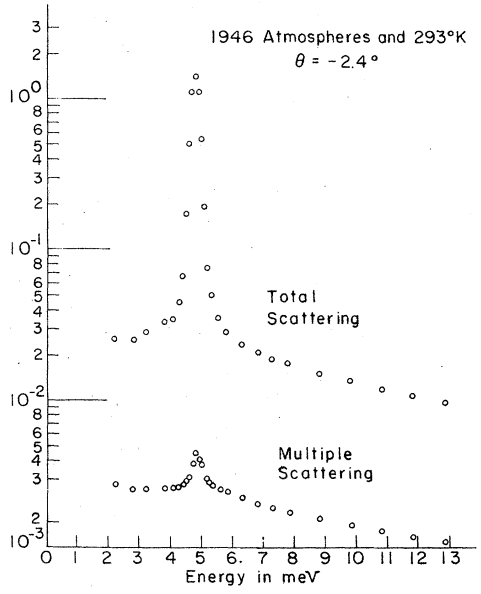


FIG. 3. Total-scattering and multiple-scattering contribution for $\rho = 1946$ atm and $T = 293$°K at a scattering angle of 2.4°. The ordinate expresses the scattering cross section $\sigma_s(E,\theta)$ at energy transfer $E$ and scattering angle $\theta$ in an arbitrary unit. The multiple-scattering part is given in proportion to the total-scattering cross section. The code used for the multiple scattering computation is called MSCAT which is a Monte Carlo code originally written by Copley (Ref. 16).

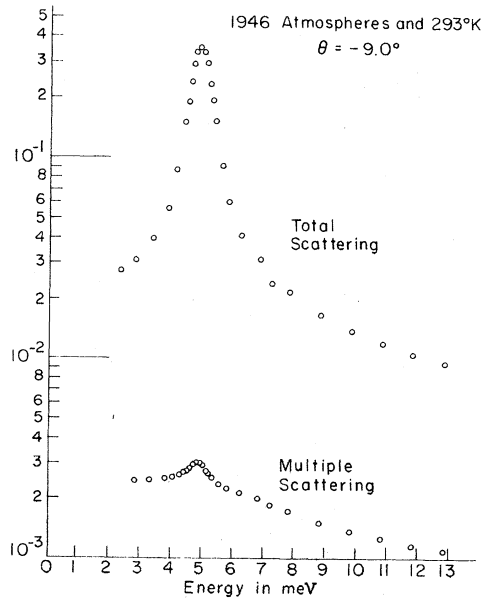


FIG. 4. Same as in Fig. 3 for a scattering angle of 9.0°.

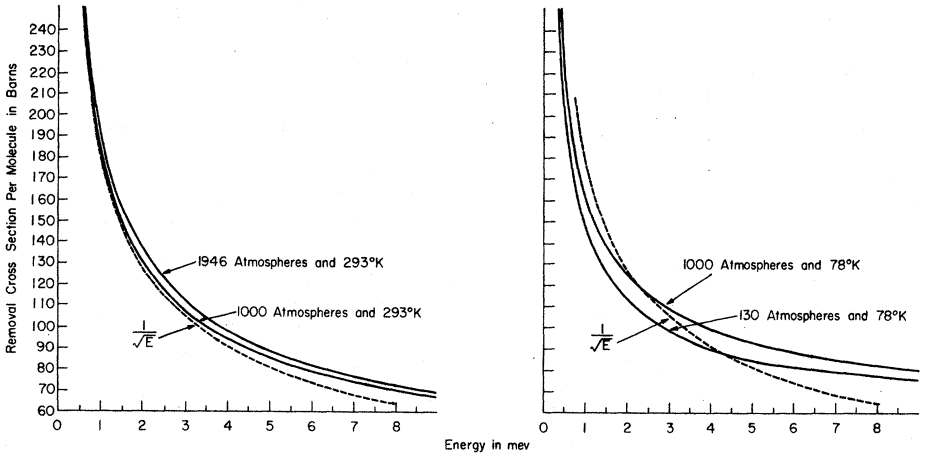


FIG. 5. Example of removal cross sections calculated as described in the text.

ing occurred and calculated the self-shielding correction using the removal cross section corresponding to the nominal ortho-para ratio.

### C. Multiple-scattering correction

In order to calculate the multiple-scattering contribution[16] it is necessary to have an estimate of $S_s(Q,\omega)$. However, it is well known that this component is rather insensitive to the details of the scattering law as long as the general features of the scattering law and the target geometry are properly treated.

We chose a model scattering function due to Nelkin and Ghatak[11] which has been shown[17] to give a reasonable representation of the scattering function for moderately dense gases. Figures 3 and 4 are typical curves showing the distribution of total and multiply scattered neutrons computed from this model. The multiple scattering amounts to less than 2% of the total scattering at all angles and is therefore insignificant compared to other uncertainties in the data. We ascribe this result to the novel design of the high-pressure container, as described in Sec. III B.

The multiple-scattering code was also used to calculate the removal cross section due to scattering. The double-differential scattering cross section [Eq. (12)] is integrated over all $Q$ and $\omega$ associated with an incident wave vector $k_i$,

$$\sigma = 4\pi a_{\mathrm{inc}}^2 k_i \int d\Omega \int d\omega\, k_f S_s(Q,\omega)\,. \qquad (16)$$

The result is shown in Fig. 5.

The multiple-scattering correction for the lower-temperature data all have basically the same feature as the results shown in Figs. 3 and 4.

## IV. RESULTS OF THE DATA ANALYSIS

We fitted the high-density data at room temperature with a Lorentzian function [Eq. (8)]. A typical result is illustrated in Fig. 6. The diffusion coefficient so obtained is accurate to about 10%. The inset in Fig. 6 shows the statistical distribution of the results obtained from the individual detector groups. For the low-temperature data, the counting statistics were better and typical fits are shown in Fig. 7. The accuracy of the diffusion coefficients obtained from fitting the low-temperature

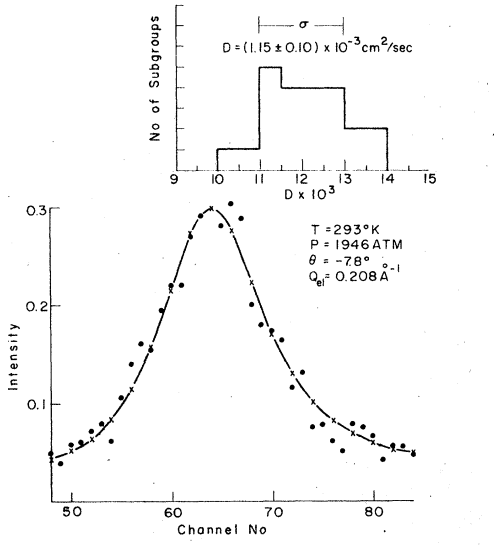


FIG. 6. Self-part of the dynamic structure factor of hydrogen gas at 293°K and the distribution of diffusion coefficients obtained by fitting a Lorentzian neutron-scattering function [Eq. (8)] to the data for the individual detector subgroups.

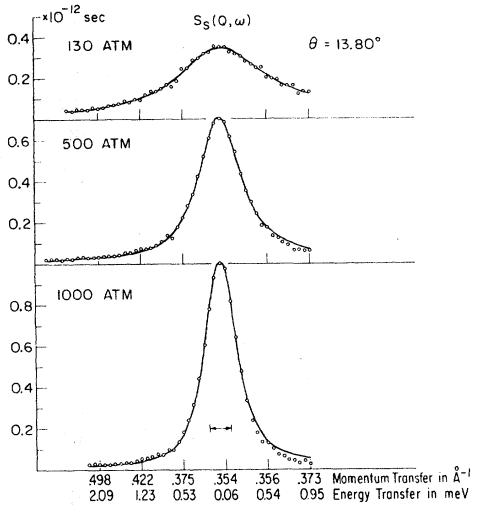


FIG. 7. Self-part of the dynamic structure factor of hydrogen gas at 78 °K. The corresponding densities are given in Table I. Note that the data are not presented in constant $Q$ form.

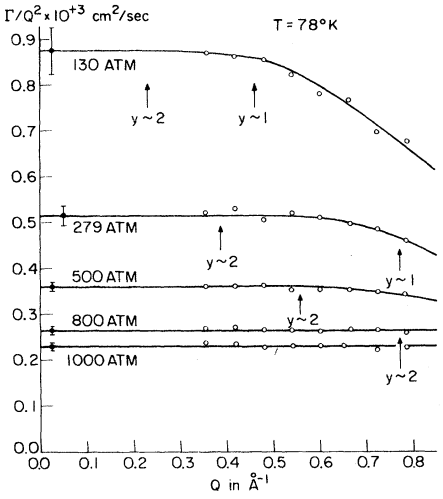


FIG. 8. Half-width at half-maximum ($\Gamma$) of $S_s(Q,\omega)$ divided by $Q^2$ as function of $Q$. For $y \geq 2$ the $\Gamma$ is expected to be accurately given by $DQ^2$. Therefore, the intercept of the solid line at $Q=0$ gives $D$.

data was typically (3–5)% of the absolute value.

Figure 8 shows the full width at half-maximum of the self-correlation function divided by $Q^2$ as a function of $Q$. The solid line indicates the extrapolation to $Q \to 0$. The open points were determined from constant angle time-of-flight data and the solid points indicate the $Q=0$ extrapolated value of the self-diffusion coefficient at each density.

Table I contains the measured values of the diffusion coefficient for three densities at room temperature and for five densities at 78 °K. The ratios of packing to close packing are listed for $r_0 = 2.57$ Å at 293 °K and $r_0 = 2.917$ Å and $r_0 = 2.958$ Å for 78 °K along with the Enskog diffusion coefficients calculated from Eq. (3) and using[18]

$$g(r_0) = (1 - 0.5\eta)/(1 - \eta)^3 . \tag{18}$$

The hard-sphere diameter of 2.917 Å was arrived

TABLE I. Summary of the experimentally measured self-diffusion coefficients and the Enskog diffusion coefficients as computed from Eq. (1). Also given are the critical- and triple-point constants.

| $T$(°K) | $P$(atm) | $n(10^{22}$ cm$^{-3})$ | $nr_0^3/\sqrt{2}$ | $D(10^{-3}$ cm$^2$/sec) | $D_E$ |
|---|---|---|---|---|---|
| 293 | 1000 | 1.49 | 0.1788 | 1.97 ± 0.19 | 1.743 |
| | 1504 | 1.89 | 0.1680 | 1.46 ± 0.13 | 1.148 |
| | 1946 | 2.14 | 0.2569 | 1.20 ± 0.10 | 0.946 |
| 78 | 130 | 1.15 | 0.2012 [a] | 0.88 ± 0.05 | 0.876 [a] |
| | | | 0.2105 [b] | | 0.858 [b] |
| | 279 | 1.74 | 0.3052 | 0.52 ± 0.03 | 0.455 |
| | | | 0.2187 | | 0.440 |
| | 500 | 2.16 | 0.3795 | 0.36 ± 0.01 | 0.303 |
| | | | 0.3957 | | 0.290 |
| | 800 | 2.55 | 0.4471 | 0.27 ± 0.01 | 0.213 |
| | | | 0.4673 | | 0.201 |
| | 1000 | 2.74 | 0.4809 | 0.23 ± 0.01 | 0.179 |
| | | | 0.5011 | | 0.169 |

$T_c = 33$ °K $\quad n_c = 0.939 \times 10^{22}$ $\quad T_t = 13.8$ °K $\quad n_t = 2.30 \times 10^{22}$

[a] For $r_0 = 2.917$ Å.
[b] For $r_0 = 2.958$ Å.

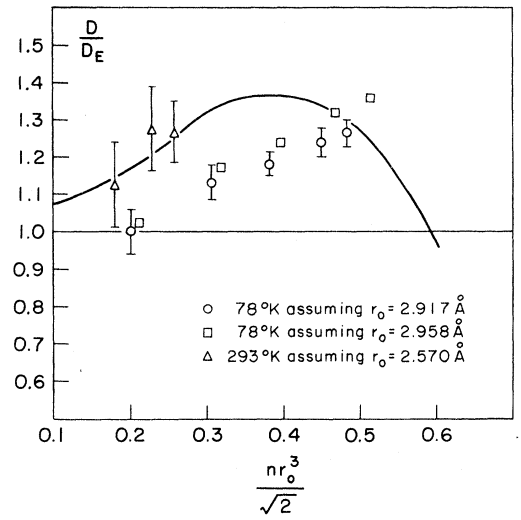


FIG. 9. $D/D_E$ plotted as function of the reduced density. The solid line is from Alder *et al.* (Ref. 1) and represents the enhancement in the case of the hard-sphere system.

at from the measured value of the low-density diffusion coefficient at 85 °K and using Eq. (6).[19] An alternative hard-sphere diameter of 2.958 Å was derived from the equation-of-state measurements of Michels *et al.*[20] The high-temperature hard-sphere diameter of 2.57 Å was derived from low-density room-temperature diffusion data.[19]

In Fig. 9 we show a plot of the ratio of the measured to the Enskog diffusion coefficients as a function of reduced density. One clearly sees enhancement over the Enskog value at higher densities. This behavior has also been observed in methane.[21] The solid line is the result of hard-sphere CMD calculations by Alder, Gass, and Wainwright.[4]

## V. CONCLUSIONS

We have measured the incoherent scattering of neutrons from gaseous diatomic hydrogen at wave vectors from $Q = 0.355$ Å$^{-1}$ to $Q = 1.00$ Å$^{-1}$. The macroscopic diffusion coefficient derived from these data shows a density dependence which differs from the hard-sphere Enskog theory. The present neutron measurements are qualitatively consistent with results obtained from computer experiments on hard spheres which indicate the existence of important dynamical effects which vary with density. Such an interpretation, however, must be viewed cautiously since the diatomic nature of hydrogen and the attractive part of the molecular potential could also account for the results reported here. However, in the context of a growing knowledge of dynamical processes in classical many-body systems,[22] it is reasonable to conjecture that the enhancement we observe is due, at least in part, to density-dependent collective effects in the surrounding medium.

---

*Work performed under the auspices of the U.S. ERDA.

†On leave of absence from AB Atomenergi, Studsvik, Sweden.

[1]B. J. Alder and T. E. Wainwright, J. Chem. Phys. 33, 1439 (1960); D. Levesque and L. Verlet, Phys. Rev. A 2, 2514 (1970); J. Kushick and B. J. Berne, J. Chem. Phys. 59, 3732 (1973); S. H. Chen and A. Rahman, J. Mol. Phys. (to be published).

[2]G. F. Mazenko, Phys. Rev. A 7, 209 (1973); 7, 222 (1973); P. M. Furtado, G. F. Mazenko, and S. Yip, *ibid.* 14, 869 (1976); P. Resibois, J. Stat. Phys. 13, 303 (1975).

[3]S. H. Chen, Y. Lefevre, and S. Yip, Phys. Rev. A 8, 3163 (1973); T. A. Postal, S. H. Chen, and K. Skold, Proceedings of the Conference on Neutron Scattering, Gatlinburg, Tenn., 1976 (unpublished), p. 862; N. J. Trappeniers and P. H. Oosting, Phys. Rev. 51, 418 (1971).

[4]B. J. Adler, D. M. Gass, and T. E. Wainwright, J. Chem. Phys. 53, 3813 (1970).

[5]B. J. Alder and T. E. Wainwright, Phys. Rev. A 1, 18 (1970).

[6]J. R. Dorfman and E. G. D. Cohen, Phys. Rev. A 6, 776 (1972).

[7]A. Rahman, Phys. Rev. 136, A405 (1964).

[8]P. M. Furtado, G. F. Mazenko, and S. Yip, Phys. Rev. A 14, 869 (1976); P. Resibois, J. Stat. Phys. 18, 303 (1975).

[9]R. Zwanzig, Phys. Rev. 133, A50 (1964).

[10]S. Chapman and T. G. Cowling, *The Mathematical Theory of Non-Uniform Gases*, 3rd ed. (Cambridge, U.P., London, 1970).

[11]M. Nelkin and A. Ghatak, Phys. Rev. 135, A4 (1964).

[12]S. H. Chen and A. Rahman, J. Mol. Phys. (to be published).

[13]V. F. Sears, Can. J. Phys. 44, 1279 (1966).

[14]R. Kleb, G. E. Ostrowski, D. L. Price, and J. M. Rowe, Nucl. Instum. Meth. 106, 221 (1973).

[15]J. R. D. Copley, D. L. Price, and J. M. Rowe, Nucl. Instrum. Meth. 107, 501 (1973).

[16]J. R. D. Copley, Comp. Phys. Commun. 7, 289 (1974).

[17]Y. Lefevre, S. H. Chen and S. Yip, *Neutron Inelastic Scattering* (IAEA, Vienna, 1972), p. 445.

[18]N. F. Carnahan and K. E. Starling, J. Chem. Phys. 51, 635 (1969); B. J. Alder and T. E. Wainwright, *ibid.* 46, 4181 (1960).

[19]*American Institute of Physics Handbook* (McGraw-Hill, New York, 1963), 2nd ed., p. 2-236.

[20]A. Michels *et al.*, Physica (Utr.) 26, 393 (1960).

[21]N. J. Trappeniers and P. H. Oosting (see Ref. 3).

[22]I. M. DeSchepper and H. Van Beyeren, Physica (Utr.) 75, 1 (1974).